透明酸化物半導体 (Ba, Sr)SnO_3 薄膜の真空熱処理による高移動度化

北海道大学　電子科学研究所　ジョ、ヘジュン

Mobility Enhancement in Transparent Oxide Semiconductor (Ba, Sr)SnO_3 Films via Vacuum Annealing

Hai Jun Cho
Research Institute for Electronic Science, Hokkaido University

La ドープペロブスカイトスズ酸化物(La-$A$$SnO_3$, A = Ba, Sr)は、新しい透明酸化物半導体として注目されている。Sn 5s 軌道からなる伝導帯と、O 2p 軌道からなる価電子帯の間のバンドギャップは可視光の最大エネルギー(3.1 eV)よりも広く、Sn 5s 軌道の大きな重なり積分により、La-$A$$SnO_3$ 単結晶は高い電子移動度を示す。しかし、薄膜成長中に構造欠陥が生じるため、La-$A$$SnO_3$ 薄膜の電子移動度は光電子デバイス応用に必要なレベルに達していない。本研究では、単純な熱処理プロセスにより、La ドープ $SrSnO_3$ 薄膜の電子移動度が向上したことを報告します。4.6 eV の広いバンドギャップとともに、約 3000 S cm^{-1} の記録的な高導電率が得られました。以上の結果から、La ドープ $SrSnO_3$ 薄膜は DUV 透明電極としての応用が期待できます。

La-doped perovskite stannates (La-$A$$SnO_3$, A = Ba, Sr) have attracted attention as novel transparent oxide semiconductors. The bandgap between the conduction band composed of Sn 5s orbital and the valence band composed of O 2p orbital is wider than the maximum energy of visible light (3.1 eV), and La-$A$$SnO_3$ single crystal exhibits high electron mobility due to large overlap population of Sn 5s orbital. However, thin films of La-$A$$SnO_3$ exhibit low electron mobility due to structural defects associated with the film growth, which strongly limits the full potential of La-$A$$SnO_3$ in optoelectronic device applications. Here I report successful mobility enhancements in La-doped $SrSnO_3$ (LSSO) films via a simple post-treating process. A record-high electrical conductivity value of ~3000 S cm^{-1} was obtained alongside a wide bandgap of 4.6 eV. The La-doped $SrSnO_3$ thin film would be applied as a DUV transparent electrode.

1. Introduction

Transparent semiconductors are essential materials for building transparent thin film transistors, which provide a platform for controlling light with electricity. Therefore, there are extensive research effort towards improving the optoelectronic properties of transparent semiconductors to transcend the performance of optoelectronic devices. Two of the most important characteristics in this regard are high optical bandgap (E_g) and electron mobility (μ), which determine the spectral range of operation and the operation speed, respectively.

This is the greatest challenge in designing the transparent semiconductor for optoelectronic applications since increasing E_g usually decreases the electrical transport properties, including μ. For example, Ga_2O_3-based materials exhibit a very large bandgap of > 5 eV, but their electrical conductivities (σ) are below 1 S cm^{-1} [1,2].

La-doped perovskite stannates (La-$A$$SnO_3$, A = Ba, Sr) can potentially overcome the typical tradeoff relationship between E_g and μ. Their conduction and valence bands consist of Sn^{5s} and O^{2p} orbitals, respectively. The large electronegativity difference between Sn and O provides a large bandgap while the disperse nature of Sn^{5s} orbitals allow rapid electron transportations. One of its kind, La-$BaSnO_3$ (LBSO), exhibits with a very high mobility of 320 cm^2 V^{-1} s^{-1} in single crystal form [3], which is even comparable to traditional semiconductors like Si [4]. However, its E_g of ~3.1 eV limits its optoelectronic operation is to visible range. Higher E_g values of > 4 eV can be achieved La-$SrSnO_3$ (LSSO), which is sufficient for transmitting UV lights. However, their electrical transport properties are poor, especially in form of thin films. The highest σ reported from LSSO to date is 1000 S cm^{-1} [5].

In our previous research, we found that the structural defects in LBSO films can be eliminated with a simple post-annealing process in vacuum, which greatly enhanced the electrical transport properties [6]. In this research, we extend the same approach to LSSO films and report the results, including a record-high σ value of ~3000 S cm^{-1} with a E_g of 4.6 eV, which can even transmit deep-UV (DUV) lights. The σ observed from the LSSO films in this work is much higher than that observed from other oxide conductors at similar E_g (Fig. 1) [1,2,7-9].

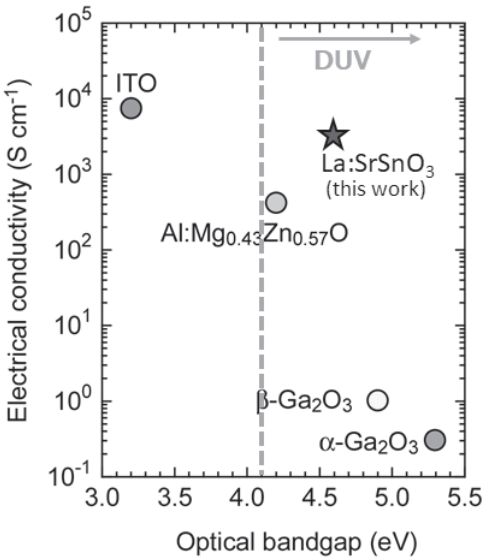

Figure 1 – Optoelectronic properties of transparent semiconductors and the results obtained from this work.

2. Experiment

$La_xSr_{1-x}SnO_3$ (x = 0.005, 0.02, 0.03 and 0.05) epitaxial films were fabricated on (001) MgO (a = 0.4212 nm) single crystal substrates using pulsed laser deposition (PLD) technique (KrF excimer). The laser parameters are wavelength (λ) = 248 nm, fluence ~2 J cm^{-2} $pulse^{-1}$, and repetition rate = 10 Hz. The substrate temperature and oxygen pressure inside the chamber during the film growth were 790 ° C and 20 Pa, respectively. High- resolution X-ray diffraction (Cu $K_{\alpha 1}$, ATX-G, Rigaku Co.) was performed to investigate the crystalline phase, orientation, lattice parameters, film thickness, and the lateral grain size of the films. Scanning transmission electron microscopy (STEM) was performed to observe the microstructures of the films. DC four-probe method in van der Pauw configuration was used to measure the σ , carrier concentration (n), and Hall mobility (μ_{Hall}) of the films. The thermopower (S) was acquired from the thermos-electromotive force (ΔV) generated by a temperature difference (ΔT) of ~4 K across the film using two Peltier

devices. The temperatures at each end of the films were simultaneously measured, and the S was calculated from the slope of the $\Delta T - \Delta V$ plot. The characterizations were repeated after the LSSO films were vacuum annealed at 790°C and 10^{-2} Pa for 30 mins.

3. Results and Discussions

The reciprocal space mappings (RSM) of the as-grown and vacuum annealed LSSO films ($x = 0.03$) are shown in Fig. 2 as an example. The 204 diffraction peaks of LSSO and MgO substrates can clearly be identified, but the epitaxial growth was not coherent as the q_x values of peaks from the film and the substrate are not the same. The vacuum annealing sharpened the LSSO peak in the diffraction pattern along q_x and decreased its integral width (Figs. 2a and 2b). All LSSO films exhibited a substantial increase in the lateral grain size (D) (Fig. 2c). According to the Scherrer's equation, expressed as $D = (\text{Integral width})^{-1}$, the largest grain growth was observed at $x = 0.03$, which changed from ~12 nm in the as-grown state to ~28 nm after vacuum annealing.

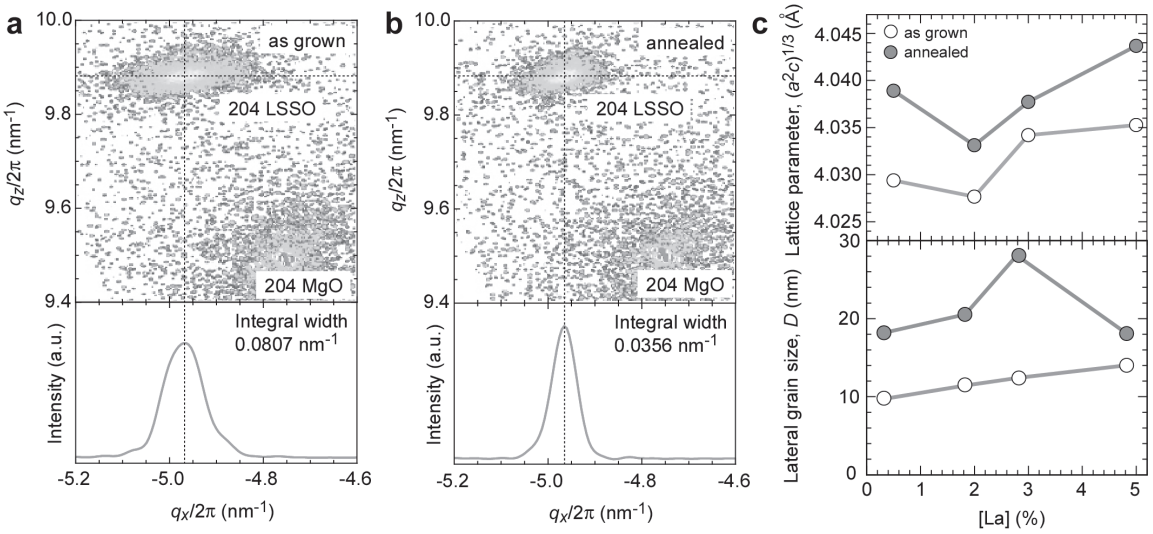

Figure 2 – (a, b) RSMs around 204 LSSO diffraction spot of (a) as grown and (b) vacuum annealed films. The cross-sectional diffraction patterns along $q_x/2\pi$ direction are shown at the bottom of each RSM. (c) Changes in (top) the average lattice parameter and (bottom) lateral grain size of the as-deposited LSSO films (white) and annealed LSSO films (red) as a function of La concentration.

The lateral grain growth after vacuum annealing was further confirmed with low-angle annular dark-field scanning transmission microscopy (LAADF-STEM). As shown in Fig. 3, columnar grains perpendicular to the film/substrate interface are observed. The vacuum annealing significantly increases the D of the LSSO film, which is in excellent agreement with the RSM results (Fig. 2). It is also shown that the strain contrast in the LAADF-STEM noticeably decreases after the vacuum annealing, suggesting that the lateral grain growth relaxes the LSSO film.

The resulting electrical transport properties at room temperature are summarized in Fig. 4. All electron transport properties (σ, n, μ_{Hall}) substantially increased after the vacuum annealing (Fig. 4a and 4b). The absolute value of S decreased after the vacuum annealing,

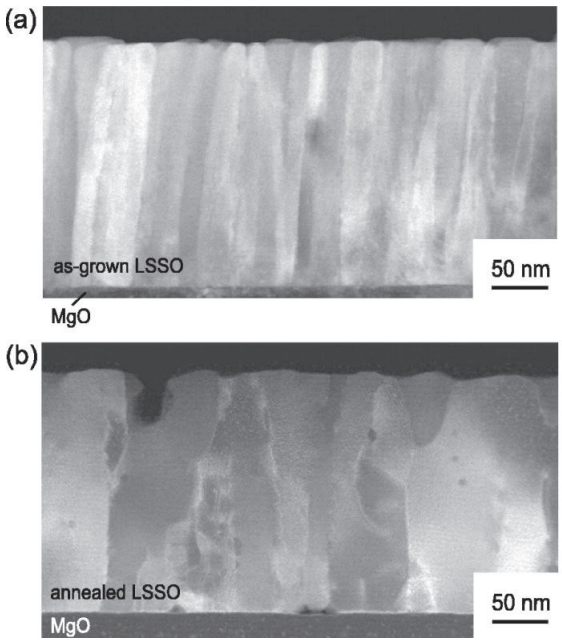

Figure 3 – Cross-sectional LAADF-STEM micrographs of (a) as-grown and (b) vacuum annealed LSSO films.

which is consistent with the changes in n. The greatest enhancement was observed at $x = 0.05$, but the highest absolute values were observed at $x = 0.03$. This is likely attributed to the fact that 5% is further away from the solubility limit of La in $SrSnO_3$ lattice.

The σ of ~3000 S cm^{-1} observed from the 3% LSSO film after vacuum annealing is a record among all reported values from LSSO. This is largely associated with the increase in n, as the change in μ_{Hall} is not substantial at $x = 0.03$ (Fig. 4 d). Considering the short vacuum annealing time, the amount of oxygen vacancy is likely small to affect the overall n, and it is reasonable to assume that the generation of carrier electrons is mostly attributed to the activation of La dopants. The 3% LSSO film has the highest La dopant activation rate (~70%) in this study, which was also accompanied by the largest grain size. In this regard, the data suggest that La dopant activation is the most critical factor for enhancing the electron transport properties of LSSO films, which is strongly affected by the lateral grain size.

The optical transmission and reflection spectra of vacuum annealed 3% LSSO film (thickness: 112 nm)

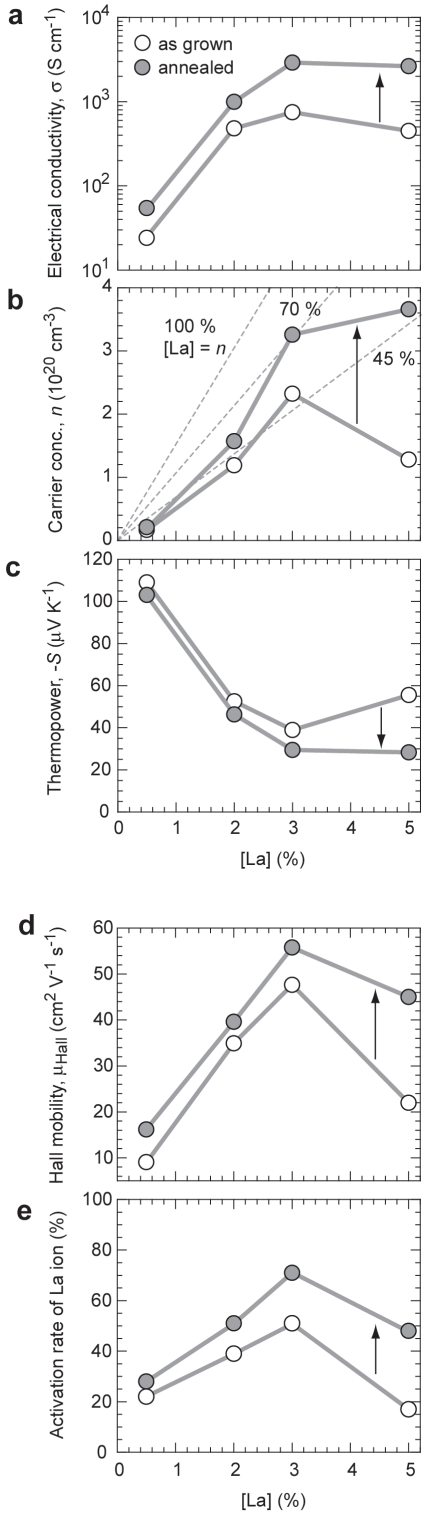

Figure 4 – Electron transport properties of the LSSO films as a function of La content (%). (a) σ, (b) n, (c) $-S$, (d) μ_{Hall} and (e) Activation rate of La dopants.

grown of double-side polished (001) MgO substrate is shown in Fig. 5 (inset). According to the $(\alpha h\nu)^2 - h\nu$ plot, the estimated E_g value is ~4.6 eV, which agrees well with previously reported values [10] and is sufficient enough to transmit DUV lights. The LSSO films examined in this research have appropriate optoelectronic properties for UV-based optoelectronic devices.

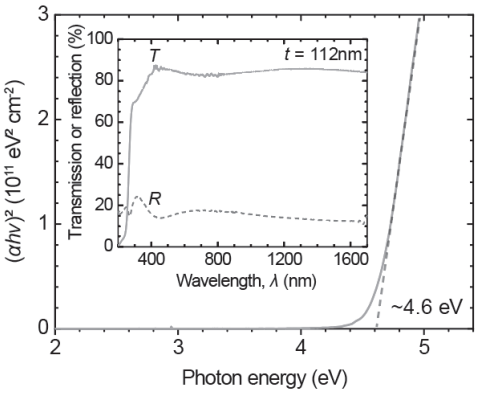

Figure 5 – Optical properties of vacuum annealed 3% LSSO film. The E_g was ~4.6 eV, which can transmit DUV lights.

4. Conclusions

In this research, LSSO films with excellent optoelectronic properties (~3000 S cm^{-1}, E_g ~4.6 eV) were successfully fabricated on MgO substrate using PLD and a simple vacuum annealing process. Structural analyses revealed that the columnar grains grow in the lateral direction during the vacuum annealing, and the lattice strain significantly gets reduced. The structural improvements also considerable improvements in activation of La dopants, which lead to enhanced the electron transport properties like high La dopant activation (~70%, 3.26×10^{20} cm^{-3}) and high Hall mobility (55.8 cm^2 V^{-1} s^{-1}). These are very promising characteristics for expanding the operation range of optoelectronic devices to UV region, as they are sufficient for UV transmitting electrodes.

Acknowledgements

The financial support from the Nippon Sheet Glass Foundation for Materials Science and Engineering is greatly appreciated by the author of this work.

References

1. T. Kawahamura, G.T. Dang, M. Furata, *Japanese Journal of Applied Physics* 51 (4) 040207 (2012)
2. R. Wakabayashi, K. Yoshimatsu, A. Ohtomo, *Applied Physics Letters* 111 (16) 4 (2017)
3. H.J. Kim, U. Kim, H.M. Kim, T.H. Kim, H.S. Mun, B.G. Jeon, K.T. Hong, W.J. Lee, C. Ju, K.H. Kim, K. Char, *Applied Physics Express* 5 (6) 3 (2012)
4. N.M. Johnson, C. Herring, D.J. Chadi, *Physical Review Letters* 56 (7) 769 (1986)
5. E. Baba, D. Kan, Y. Yamada, M. Haruta, H. Kurata, Y. Kanemitsu, Y. Shimakawa, *Journal of Physics D: Applied Physics* 48 (45) 455106 (2015)
6. H.J. Cho, T. Onozato, M. Wei, A. Sanchela, H. Ohta, *APL Materials* 7 (2) 022507 (2019)
7. M. Orita, H. Ohta, M. Hirano, H. Hosono, *Applied Physics Letters* 77 (25) 3 (2000)
8. C.G. Granqvist, A. Hultaker, *Thin Solid Films* 411 (1) 5 (2002)
9. D. Zhang, W. Zheng, Q.H. Zheng, A.Q. Chen, X. Ji, F. Huang, *Advanced Electronic Materials* 2 (11) 1600320 (2016)
10. D.J. Singh, Q. Xu, K.P. Ong, *Applied Physics Letters* 104 (1) 011910 (2014)